

UNCLASSIFIED

AD NUMBER

AD529085

CLASSIFICATION CHANGES

TO: unclassified

FROM: secret

LIMITATION CHANGES

TO:

Approved for public release, distribution unlimited

FROM:

Distribution authorized to U.S. Gov't. agencies only; Test and Evaluation; JAN 1974. Other requests shall be referred to Director, Naval Research Laboratory, Washington, DC 20375.

AUTHORITY

31 Dec 1993, per document marking; NRL Code/5309 memo dtd 20 Feb 1997

THIS PAGE IS UNCLASSIFIED

SECRET

NRL Memorandum Report 2701
Copy ~~20~~ of 175 Copies

AD529085

Radar Ionospheric Propagation Effects Determined from One-Way Path Tests

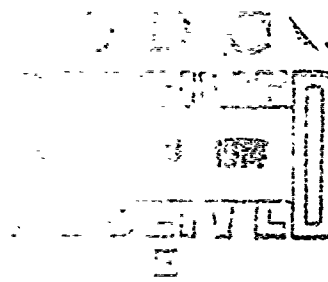
[Unclassified Title]

D. B. TRIZNA AND J. M. HUDNALL

*Radar Techniques Branch
Radar Division*

January 1974

ALL INFORMATION CONTAINED
HEREIN IS UNCLASSIFIED EXCEPT WHERE SHOWN
OTHERWISE



NAVAL RESEARCH LABORATORY
Washington, D.C.

DOC CONTROL
NO. 40561

SECRET

SECRET, classified by DIRNRL.
Exempt from GDS of E.O. 11652 by DIRNRL.
Ex. Cat. (3). Auto. declass. on Dec. 31, 1993

Distribution limited to U.S. Government Agencies only; test and evaluation; January 1974. Other requests for this document must be referred to the Director, Naval Research Laboratory, Washington, D.C. 20375.

SECRET

NATIONAL SECURITY INFORMATION

Unauthorized Disclosure Subject to Criminal Sanctions.

SECRET

SECRET

SECURITY CLASSIFICATION OF THIS PAGE (When Data Entered)

REPORT DOCUMENTATION PAGE		READ INSTRUCTIONS BEFORE COMPLETING FORM
1. REPORT NUMBER NRL Memorandum Report 2701	2. GOVT ACCESSION NO.	3. RECIPIENT'S CATALOG NUMBER
4. TITLE (and Subtitle) RADAR IONOSPHERIC PROPAGATION EFFECTS DETERMINED FROM ONE-WAY PATH TESTS (U)	5. TYPE OF REPORT & PERIOD COVERED An interim report, work is continuing.	
	6. PERFORMING ORG. REPORT NUMBER	
7. AUTHOR(s) Dennis B. Trizna and James M Hudnall	8. CONTRACT OR GRANT NUMBER(s)	
9. PERFORMING ORGANIZATION NAME AND ADDRESS Naval Research Laboratory Washington, D.C. 20375	10. PROGRAM ELEMENT, PROJECT, TASK AREA & WORK UNIT NUMBERS 53R02-42 USAF MIPR FY76207300001	
11. CONTROLLING OFFICE NAME AND ADDRESS Department of the Air Force Electronic Systems Division	12. REPORT DATE January 1974	
	13. NUMBER OF PAGES 34	
14. MONITORING AGENCY NAME & ADDRESS (if different from Controlling Office)	15. SECURITY CLASS. (of this report) SECRET	
	15a. DECLASSIFICATION/DOWNGRADING SCHEDULE XGDS-3-1993	
16. DISTRIBUTION STATEMENT (of this Report) Distribution limited to U.S. Government Agencies only; test and evaluation; January 1974. Other requests for this document must be referred to the Director, Naval Research Laboratory, Washington, D.C. 20375.		
17. DISTRIBUTION STATEMENT (of the abstract entered in Block 20, if different from Report)		
18. SUPPLEMENTARY NOTES		
19. KEY WORDS (Continue on reverse side if necessary and identify by block number) Ionospheric propagation Noise measurement HF Radar		
20. ABSTRACT (Continue on reverse side if necessary and identify by block number) (Secret) On 9, 10, 11 November 1972, one-way HF transmission tests from Cyprus to England were run to determine the effect of the ionosphere in possible contamination of a transmitted clean spectrum. The results presented herein yield a lower limit on such contamination, and indicate that sources other than forward propagation mechanisms (scintillation, multipathing, forward scatter from electron density irregularities, etc.) are responsible for the contamination of two-way clutter spectra.		

DD FORM 1 JAN 73 1473

EDITION OF 1 NOV 65 IS OBSOLETE
1

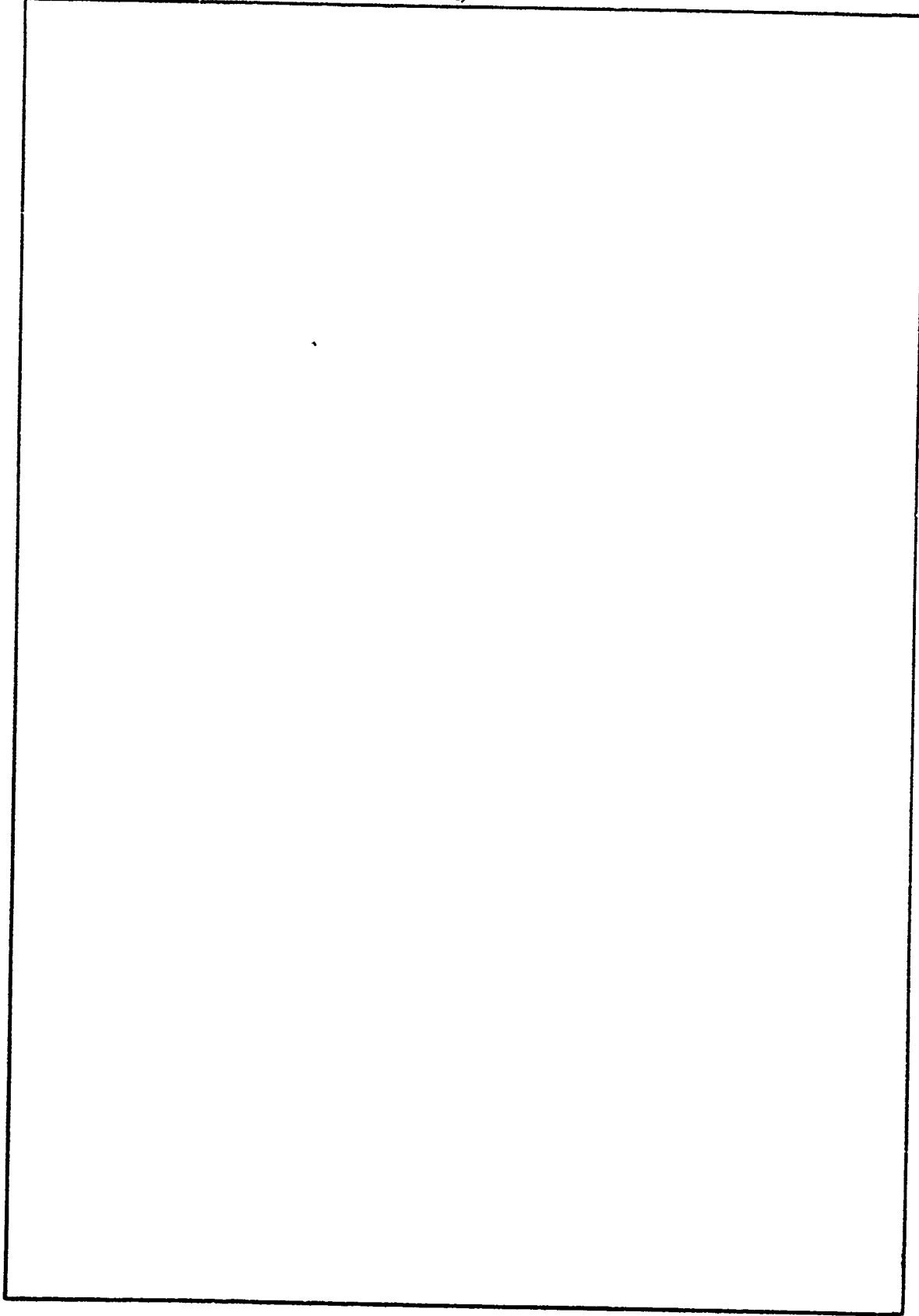
(Page ii is blank)

SECRET

SECURITY CLASSIFICATION OF THIS PAGE (When Data Entered)

SECRET

SECURITY CLASSIFICATION OF THIS PAGE(When Data Entered)



SECRET

SECURITY CLASSIFICATION OF THIS PAGE(When Data Entered)

SECRET

TABLE OF CONTENTS

	<u>Page</u>
Abstract	iv
I. INTRODUCTION	1
II. TEST CONFIGURATION AND PROPAGATION GEOMETRY	2
III. DATA ANALYSIS TECHNIQUES	2
A. Doppler Spectra	2
B. Short-Term Signal-Noise Correlation	3
IV. ANALYSIS OF OTH DATA	4
A. Time-Averaged Coherent Spectra	5
B. Short-Term Signal-Noise Corelation Behavior	6
V. SUMMARY AND DISCUSSION	9
VI. REFERENCES	11
APPENDIX I	12

DOC CONTROL
NO 40561

SECRET

ABSTRACT
(Secret)

On 9, 10, 11 November 1972, one-way HF transmission tests from Cyprus to England were run to determine the effect of the ionosphere in possible contamination of a transmitted clean spectrum. The results presented herein yield a lower limit on such contamination, and indicate that sources other than forward propagation mechanisms (scintillation, multipathing, forward scatter from electron density irregularities, etc.) are responsible for the contamination of two-way clutter spectra.

* * *

This report represents work performed by the Naval Research Laboratory (NRL) to carry out for the U. S. Air Force the investigation of certain Over-the-Horizon (OTH) techniques using the AN/FPS-95 Radar. This Research and Development (R&D) work was conducted by NRL in direct technical support to the Over-the-Horizon Program Office (OCS) of the Electronic Systems Division (AFSC).

SECRET

RADAR IONOSPHERIC PROPAGATION
EFFECTS DETERMINED FROM ONE-WAY PATH TESTS
(Unclassified Title)

IONOSPHERIC PROPAGATION EFFECTS
DETERMINED FROM AN/FPS-95 ONE-WAY PATH TESTS
(Secret Title)

I. INTRODUCTION (U)

(S) An implicit assumption in the design of a 90-dB dynamic range OTH Doppler radar is that the ionosphere will provide a transmission path of equivalent dynamic range or better. Experiments run at MADRE, with a useful dynamic range of 65 to 70 dB indicated that, except for occasional long-range meteor spectral bursts, this assumption was valid. As the AN/FPS-95 radar came into operation under the DVST program it became apparent that some agent was introducing noise across the 40-Hz spectrum, 65 to 70 dB below peak clutter, which consequently prevented achievement of desired target-to-noise ratios. A comprehensive hardware test program, run parallel with DVST, was begun in early June 1972, by NRL, MITRE, and RCA DVST personnel to search for possible hardware sources of "Clutter-Related Noise" (CRN). Various equipment problems were found and corrected, particularly in the antenna field. Later LOS transmit and receive tests indicated that, except for some evidence of element vibrational spectrum contamination for frequencies below 17.5 MHz, the system did not appear to be responsible for the level of spectral noise observed in the monostatic backscatter from long range. R. Rafuse¹ has argued that LOS tests do not provide the angular spread, both in elevation angle and azimuth, that one-way paths and two-way backscatter provide. These arguments are based upon a ray treatment of the problem and will not be considered further, as tests have been designed to circumvent this problem.

(S) As a result of the apparent cleanliness of the hardware at high frequencies it was decided to test the next component of the radar system, the transmission medium, on a one-way path. The only signal source with sufficient transmit power and spectral purity that could be made available at reasonable notice and cost was the COBRA SHOE system, located on Cyprus, 1760-nmi ground range from COBRA MIST.

(S) These tests were carried out over a three-day period the week before the Technical Advisory Committee meeting of November 1972; this meeting resulted ultimately in the official end of DVST/IOT&E and a redirected effort under the Scientific Advisory Committee. The results are presented because they do set a lower limit on contamination by the possible propagation agents in the ionosphere, e.g., forward scatter from F-region electron density irregularities, dispersion, ionospheric heating, etc. This measured limit does not appear to be of a level responsible for CRN. However, because it was a one-way path, the test does not preclude ionospheric backscatter from over-dense meteor trails and D and E region irregularities at

SECRET

long range as noise sources for the monostatic two-way path. In addition, because of the 1760-nmi ground range from Cyprus, it does not preclude noisy secondary paths by forward scatter from meteor trails and other density irregularities at D and E region heights, familiar in VHF scatter communications, since these paths are not available at such long range on a one-hop basis. All of these potential agents are natural in origin. Man-made causes (such as vibrating power lines, automobile and train traffic, etc.) inherent in the backscatter mechanism are now being considered as well in a comprehensive analysis of the problem of Clutter-Related Noise.

II. TEST CONFIGURATION AND PROPAGATION GEOMETRY (U)

(U) The propagation geometry is shown in the 3-D ray trace of Figure 1, which uses a spacial grid of predicted ionospheres for the ionospheric model.

(S) The signal source was a CW signal which was keyed off for a two-minute period after each four-minute transmission, to establish the ambient noise floor. The signal was transmitted via a side lobe of a rhombic antenna array, since the main lobe was not steerable to our azimuth. Based upon 400-kW transmit power, 18-dB gain per COBRA MIST antenna string, 14-dB ionospheric loss at 2°, and received signal of -43 dBm, an effective side-lobe gain of -3 dB over isotropic is estimated for the observed side lobe of this antenna. The transmitted spectrum, measured at the transmitter output with a ten-Hertz filter is shown in Figure 2.

(U) The receive site plan was to alternate between one string of the system antenna and a second test antenna, and feed into the receive chain for data taping and off-line SIGMA 5 analysis.

(U) The test antenna was a broadband fan dipole, designed by O. Woodward of RCA. It was positioned on the sea wall 15 feet above the sea wall, hence roughly 35 feet above mean tide. The sea surface is used as a ground screen for paths east from this point.

III. DATA ANALYSIS TECHNIQUES (U)

(U) As a point of reference, and to introduce the analysis tools, we consider the spectra of two synthesizer signals input at the COBRA MIST receiver. The signals pass through the entire receive chain, to A/D conversion. The digitized signals are then taped, for playback and SIGMA-5 analysis, and sent on to the hardware processor. All analysis presented herein is SIGMA-5 analysis via the NRL software processor and additional postprocessing techniques.

A. Doppler Spectra (U)

(S) Figure 3 is a spectrum of an H.P. synthesizer signal. The integration time used is 25.6 seconds, \cos^2 time weighted, a 4096 point FFT at 160

SECRET

PRF. Twenty integration periods were averaged for this spectrum. The peak signal occurs at +10 Hz, offset to show the D.C. offset and image. The image, due to random phase variation between the sum and quadrature channels, is at -10 Hz, 45 dB down from the main signal, 10 dB better than contract specification. The peak at 0 Hz is the D.C. offset in the A/D converter, which is not normally monitored because it is clutter filtered for on-line analysis by the RCA processor. The hum lines are 60 Hz on either side of the carrier, along with other harmonics, all greater than 90 dB down from the peak signal. Note that there are harmonics 70 Hz either side of the peak value at +80 and -60 Hz. These cannot be higher order harmonics of the 60-Hz lines since those will always lie at the odd ten-Hertz frequencies when folded. They are not processor induced as can be seen in Figure 4, an identical spectrum analysis run on a John Fluke synthesizer, in which the 60-Hz lines are seen, along with higher harmonics, spaced by 20 Hz. The lines at 70 Hz about the peak are not seen in this spectrum. Note that the noise floor 80 Hz from the peak is more than 10 dB below that from the Hewlett-Packard. The spectrum of the Fluke is flatter over a wider portion of the spectrum as well. The transmitted signal from COBRA SHOE used a Hewlett-Packard synthesizer, so that these results will be pertinent in later analysis.

B. Short-Term Signal-Noise Correlation (U)

(U) The second feature of the OTH data which we shall find important is the short-term correlation of peak signal and RMS noise in a Doppler window removed from the peak. Figure 5 is a Calcomp plot of a postprocessing technique in which mean noise values in any two specified Doppler windows, and peak signal in a third window, are calculated and plotted as a function of time, one point per coherent integration period (.8 sec here). In this case the peak has been chosen from the window 5 to 15 Hz, and represents the peak of the synthesizer spectrum. The noise windows are at -14 to -19 Hz, and -61 to -66 Hz. The noise calculation is simply the linear mean of all filter outputs within the window and is expressed in dBm, i.e., the equivalent level at which a coherent signal of the same value in dBm would have a signal-to-noise ratio of unity. The value of the equivalent Gaussian white noise at the receiver front end, in dBm/Hz, is simply this value minus the log of the coherent processing time, plus the log of the ratio of PRF to receiver bandwidth, to account for the ambiguous folding due to the pulsed system. The linearly averaged values of the peak and noise taken over the time displayed is also given in the information below the figure, as well as the variance of each.

(U) Four correlation coefficients of the set of noise samples versus the peak amplitude are also calculated over the entire time interval and are displayed also. One defines the correlation coefficient of one random process, $x(t)$, versus a second random process, $y(t)$, as

$$R_1 = \frac{\sum_1^N (x_1 - \bar{x}) (y_1 - \bar{y})}{\sigma_x \sigma_y N}$$

SECRET

where the σ terms are the standard deviations of the two processes and the barred values are their means. One can also define three other correlation coefficients, R_2 , R_3 , and R_4 , for the same processes: R_2 , as the first except that the magnitude of the y factor is taken in the sum; R_3 , as the first except that the magnitude of the x factor is taken; R_4 , as the first except that the magnitudes of both terms are taken before multiplying. R_4 represents the largest value that R_1 could have for the period. R_2 is useful, for example, for determining if transient effects are present. (If sharp spikes of amplitude both greater than and less than the mean amplitude value are present in near equal number, one would expect a rise in overall spectrum and hence in the "noise floor" in the windows, for each type of spike. The correlation coefficient, R_1 , would be near zero if the positive and negative spikes were equally distributed in time. The correlation coefficient, R_2 , would reflect this transient correlation, however, given x as the noise variable and y as the amplitude variable. The coefficient, R_3 , is defined for symmetry and is useful in other work.)

(U) The data displayed in Figure 5 then is the behavior in time of the peak amplitude and noise levels, in specified windows, of the H.P. synthesizer, using an integration time of .8 seconds. Results show a mean signal level over the two-minute period of -23.2 dBm, 0.00 dB variance, time averaged noise levels of -108.2 and -114.2 dBm in the indicated doppler windows, with variances over the period of 4.3 and 2.7 dB, respectively. Resultant peak signal to noise ratios over the period are 84.9 and 91.0 dB, respectively. The normal correlation coefficients, R_1 , are negligible; R_2 and R_3 are different from one another in magnitude, the asymmetry indicating a "transient" like effect discussed earlier. R_2 is close to the highest possible value, R_4 , in the first case as well.

(U) A similar display for the Fluke synthesizer is shown in Figure 6. It can be generally described as 8 dB less noisy in frequencies removed from the peak, and as having a flatter spectrum than the H.P. synthesizer, in agreement with the spectra of Figures 2 and 3.

IV. ANALYSIS OF OTH DATA (U)

(U) The techniques described in the previous section are now applied to the one-way ionospheric path data. Data taken with both the system antenna (single string) and dipole reference antenna are compared using both techniques.

(U) The combination of four-minute transmit periods and data breaks due to the ten-minute data tapes in the FPS-95 processor which run continuously presented a situation such that two-minute periods were the optimum for comparison of most of the data. All of the data were reviewed for contamination by other CW users sweeping across the spectrum and forward scatter from numerous aircraft, either locally or at the transmit site. It was found that the data on each antenna were self consistent and showed different characteristics. Two of the best examples of each are reviewed using different processing parameters to bring out the different features.

SECRET

A. Time-Averaged Coherent Spectra (U)

(U) Figures 7 and 8 represent example spectra for the system antenna and test dipole, respectively. Each spectrum is the ensemble average of four time-contiguous coherent spectra, each of 25.6 seconds coherent integration time (4096 point FFT at 160 PRF). The spectrum peak and image are at -40 and +40 Hz, respectively. The D.C. offset of the COBRA MIST system again appears at 0 Hz.

(U) On each of the spectra there is evidence of spurs roughly 60 dB down and further from the spectrum peak. These are thought to be either associated with the transmitter or are multipath contributions. The signal on a single string of the system antenna appears relatively clean down to 78 dB below peak at which time it begins to broaden. The spectral peak ten Hertz to the left of the main peak on the dipole antenna was identified with an aircraft track on the doppler-time plots generated. The CW spectrum in this case begins to broaden 70 dB from the peak. The aliased 50-Hz multiples of COBRA SHOE appear at 10 and 70 Hz, 60 and 20 Hz, -50 and -30 Hz, etc. The 60-Hz lines of the COBRA MIST system are expected, accounting for aliasing, as follows: ± 60 Hz at 20 and 60 Hz; ± 120 Hz at 80 and 0 Hz (along with the D.C. offset); ± 180 Hz at -20 and -60 Hz. All other 60 Hz multiples will occur at these frequencies as well.

(S) The interesting differences between the two spectra are the contributions on the system antenna at -4 and -76 Hz, ± 36 Hz about the peak. On the dipole spectrum there are contributions ± 40 Hz, which are probably too wide and large to be due to the 120-Hz power lines. Blower motor lines transmitted by COBRA SHOE on days 314 and 315 appeared at about ± 24.5 lines, but remained fixed in frequency throughout testing. The lines presented here are quite different in frequency, considering the ten-minute difference in time, and are probably vibrational resonances of the two antennas. Similar lines appeared throughout the three-day period, but varied in frequency and were quite often contaminated by aircraft reflections. Note that the lines at ± 36 Hz would alias to ± 4 Hz when operating at 40 PRF and would contaminate the spectrum some 75 dB down. This is not large enough to account for CRN, however, at the present level.

(U) The mechanism expected to generate such discrete contributions, as pointed out by R. Rafuse^{1&2}, are Kharman Vortex resonances, which require winds blowing perpendicular to the axis of the cylindrical dipole elements of the log periodic system antenna. Only those elements whose physical dimensions satisfy the resonance condition for a given wind velocity are expected to vibrate, accounting for a possible operating frequency, azimuthal, and polarization dependence. That is, if the vibrating elements are not a part of the active region of the antenna for a given operating frequency, their effect will not be seen in the spectrum. Similarly, vertically polarized elements will be able to be excited by winds from any direction, since they always satisfy the axis-to-wind perpendicularity requirement. Hence the effect should be seen on

SECRET

vertical polarization if the wind is sufficiently strong. Finally, an azimuthal dependence will occur on horizontal polarization, since only those strings parallel to the wind can be excited.

(S) The TOBRA SHOE transmission was not monitored line-of-sight, and it is difficult to tell whether the noise that is seen in these spectra is ionospherically induced or is actually transmitted. One should note that even if the transmitted spectrum is cleaner than that of Figure 7, effective contamination can result due to a multiplicity of paths. That is, a Gaussian distribution of paths with slightly different doppler frequencies will result in a broadened spectrum peak relative to that of the synthesizer spectra presented earlier. The noise floors of these multiple paths will add differently than the spike portion because of common overlap in the skirts. An estimate of the expected degradation due to this mechanism would require a detailed analysis of the frequency dependence of the skirt behavior. Suffice it to say that the ionosphere will support at least 25.6 seconds of coherent integration without spectrum breakup on a single path, better than 75 dB clean within ± 5 Hz. On none of the three days of operation was propagation significantly worse than this. Additional tests are planned, with line-of-sight transmission monitoring, to determine whether these limits are actually lower.

B. Short-Term Signal-Noise Correlation Behavior (U)

(U) Figures 9 and 10 present the time history of the peak signal amplitude and mean noise levels described earlier, for signals received on one string of the system antenna and the reference dipole, respectively. A key break is included in each case, during which the transmit signal was reduced by 40 dB. A number of outstanding differences are observed between the two displays: (a) different fading structure of peak signal, (b) definite correlation between noise and peak signal in one case, and (c) lack of a drop in noise level during key break in the second case. Each of these is now treated in turn. (Note: the correlation coefficients, time averages and variances are not meaningful in these figures because of the key break.)

(U) The fading structure difference is thought to be due to a combination of elevation angle pattern and cross-polarization isolation differences in the two antennas. In the case of the system antenna, signal cancellation between two paths may be occurring, causing the deep nulls. The high cross-polarized isolation of the system antenna (25 to 35 dB by spec) does not allow the residual components cross-polarized to the antenna to contribute a significant amount if they are large. Hence nulls as deep as 25 dB may be expected if the contributions from the two (or more) low angle paths which are copolarized with the system antenna cancel identically. In the case of the test dipole, more paths are probably available because of the broader elevation angle pattern on this antenna, as well as probable poorer cross-polarization isolation. Hence any nulls in power by multipath cancellation as described above will not be as deep. In addition to the lack of deep nulls, the signal from the test antenna appears to vary from one integration period to the next or faster. This is thought to be a modulation by energy reflected from moving

SECRET

facets on the sea surface. (The coherent Bragg-scatter mechanism is not effective at low forward scattering angles.)

(U) The second feature, the high correlation of noise and peak signal fading is shown in greater detail in Figure 11, a shorter period which contains no key break, so that the correlation coefficients and averages displayed are valid. The high correlation of noise with signal indicates that the noise is multiplicative in nature. Various possibilities for the source of such noise will be discussed later.

(U) Consider now the third feature mentioned earlier - the lack of a drop in noise floor during the key break when observed on the fan dipole, in addition to the lack of correlation in time of noise with peak signal. A period on the dipole equivalent to Figure 11 is shown in Figure 12. At first glance it appears that this observation, coupled with the previous figure, presents incriminating evidence in favor of the system antenna as the source of the multiplicative noise observed. However, observe that signal-to-noise ratios observed on the test dipole are not as high as those on the system antenna, and that the noise level on the dipole antenna is the same as that observed on the system antenna during key break. Hence there is not sufficient signal level on the test dipole antenna to bring up the multiplicative noise if it does exist.

(S) A subtle technique can be used to improve the situation, since we are processing a CW signal with a gated processor, and can provide information as to the bandwidth of the noise. If the noise observed is Gaussian, white noise, its effective bandwidth will be that of the receiver front end, 5 kHz. Since the sample rate of the ADC's of the sum and quadrature channels is less than this (4 kHz), each noise sample in succession will be nearly statistically independent. (Note that we are referring to each sample in succession at the 4-kHz rate, not that for a given range bin, which is sampled at the PRF, 160 in this case.) Although we cannot CW process the receive data at the 4-kHz rate because this rate is not available continuously (a sample is dropped each PRF), we can process at the normal PRF rate, after first averaging up to 24 contiguous 4-kHz samples to form a single pseudo range bin. (The twenty-fifth sample is dropped at 160 PRF.) We are essentially incoherently averaging each of N subsets of M samples (M up to 24 per subset) before performing a single N-point FFT. (One can get an improvement with pulsed data as well by averaging N subsets of M samples if the coherent signal of interest is M samples long. This is the philosophy in the range bin formation of the hardware RCA processor, $M \leq 4$.) At any rate, if the noise is truly Gaussian and white, the noise power will add linearly with M samples, while the coherent signal power should add like M^2 . (One must also consider the added loss due to not accounting for the change of phase of the CW from one sample to the next. Assuming the CW is unambiguous to within $\pm PRF/2$, from Appendix 1 this added loss due to an offset of $PRF/4$ in doppler is 1 dB in going from one to twenty samples averaged to form a bin. Hence, in this case, a gain of roughly 12 dB should be realized using this technique.)

SECRET

(U) Results for such processing on the same data periods shown in Figures 11 and 12 are given in Figures 13 and 14. Comparing Figure 14 with 12, at best a 7-dB signal-to-noise improvement is achieved in each window on the fan dipole in going from a one-sample bin to a twenty average. This improvement indicates the dominant noise floor was white; the lack of achievement of the predicted gain indicates that the narrowband noise is contributing substantially now. Comparing Figures 13 and 11, the signal received via the system antenna, no gain in signal to noise is achieved in the window nearest the peak, and only a 3-dB gain is achieved in the window farthest from the peak. Apparently the dominant noise in this case was not white, but narrowband.

(U) Considering the correlation coefficients, a definite correlation began to appear on the dipole antenna when the 20 samples were averaged. In the case of the system antenna, higher correlation was also seen in going from one to twenty averaged samples, although the correlation was extremely high to begin with. At any rate, in the case of the fan dipole the correlation coefficients do rise with application of the incoherent averaging of samples before processing. This implies that the low level narrowband noise associated with the dipole antenna is multiplicative as well.

(U) Note that although the signal-to-noise ratio in the window nearer the peak for the dipole antenna is within a dB of that for the system antenna for the twenty-sample bin, the correlation coefficients still differ markedly for the two cases. This could mean one of two things: first, that the narrowband noise associated with each antenna is inherently different in nature; or, second, that the white noise is still contributing significantly in the case of the dipole, keeping the correlation coefficients relatively low. Intuitively, one would feel that the transition from white noise dominant to narrowband noise dominant would not occur in a step-like manner upon application of the averaging technique, and that the second of the above two possibilities is probably correct.

(U) Consider finally the effects of increasing the integration time by 9 dB for each of the above cases (.8 sec to 6.4 sec). Results are shown in Figures 15 through 18. On the system antenna, in extending the integration time for both the single-sample bin and the twenty-sample bin, an increase in signal to noise of from 9.1 to 9.4 dB was achieved in the two windows. For the fan dipole, the numbers varied from 8.7 to 8.8. A 9-dB increase is what one would expect if the noise were additive, white, and time stationary.

(U) In considering the noise alone, calculations show that it is not ergodic - e.g., mean and higher moments in time averages of a single doppler bin are far different than means and higher moments for any fixed time for an ensemble of doppler bins. Hence, if one were attempting to detect a fixed amplitude signal, one would not get an improvement in signal to noise proportional to integration time. However, because the peak signal and noise are so highly correlated in time, the expected increase in signal to noise does occur here. The noise is ergodic "relative to the clutter peak." In the

SECRET

case of bistatic clutter, one observes that the noise again is not ergodic in an absolute sense, nor relative to the clutter, i.e., it is not highly correlated with fading of the clutter. In this case, it has been observed that increase of signal to noise with integration time behaves in an erratic manner. The exact behavior of the clutter case has not been investigated extensively.

(U) To recapitulate, three conclusions can be drawn from the above data comparisons: first, if no improvement in signal to noise results when applying the sample averaging technique, one can conclude that the dominant noise contribution is narrowband noise; second, if the correlation coefficient of the time variation of noise level versus peak signal level is high, the dominant noise is multiplicative. Finally, a linear increase in signal to noise with increase in integration time results, as expected if the noise were ergodic. This results because of the fact that the noise and peak signal are highly correlated even though the noise was found to be nonergodic in an absolute sense.

V. SUMMARY AND DISCUSSION (U)

(S) We have processed signals propagated on an one-way east-west OTH path over a ground range of 1760 nmi. The signals were received on a vertically polarized test dipole and a single string of the AN/FPS-95 antenna, in turn. Two aspects of the processed data were compared for each, their power spectra and their short-term behavior. Two types of anomalous spectral contributions were observed: secondary discrete spectral peaks and a narrowband, multiplicative noise floor; neither of these were of sufficient magnitude to explain the Clutter-Related Noise observed in the case of monostatic backscatter. The discrete lines were in the proper frequency range to be accounted for by Kharmon vortice wind resonances of dipole elements used in the log-periodic system antenna. The narrowband noise was found to be highly correlated in time with the variation of the received signal peak on both the system antenna and the fan dipole, although much more highly on the system antenna. It is not known whether this difference in correlation is due to a different noise generation mechanism in each of the two antennas, or whether the noise source was elsewhere, and signal level was insufficient in the test antenna to allow the narrowband noise to fully dominate the white band ambient noise which was found present in this case. Although the noise was nonergodic in a strict sense, the expected increase in signal to noise was achieved with increase in integration time because of its correlated behavior.

(S) The narrowband multiplicative noise is not of sufficient magnitude to fully explain the Clutter-Related Noise observed in monostatic operation. However, it may be the next "layer of the onion," and it is worthwhile to speculate as to what the source of this noise is. As discussed earlier, vibrational noise will generally present secondary discrete spectral peaks. An ensemble of nonlinear ground screen joints could be responsible for such multiplicative noise, and might explain the difference in magnitude of cross-correlation coefficient between the two antennas. In line-of-sight tests

SECRET

which were conducted, signal amplitudes were varied to simulate fading clutter only once, but data were not taped so that processing of the type done here was not possible.

(U) If the measured signal-related noise is ionospherically induced, some statements can be made as to its nature. First, it cannot be due to multipathing along paths far removed from those of the main signal, e.g., sidescatter from meteors. This kind of propagation would not show the high correlation of noise with peak signal that is observed here. This is not to say that such effects would not be possible in the case of monostatic ground clutter. Other ionospheric effects possible for the limit observed here might be forward scattering or scintillation from underdense meteor trails and ionospheric irregularities. Ionospheric modification is not considered as a possibility here because of the low transmitted energies in the direction of propagation used, and the low elevation angles encountered.

(U) Finally, one must consider the transmitter site for possible noise sources. Although a spectrum taken at the transmitter site provided, the signal from the transmit antenna was not monitored during the test. In addition, the energy was delivered via a sidelobe, away from the normal direction of propagation. If noise sources in the transmit antenna were present, even at a sufficiently low level so as not to be seen via the main lobe under normal operation of that system, the noise might be expected to be more dominant a contribution via a sidelobe, and even more so near a null. In addition other communications antennas at the transmit site, which point to the UK, would not have an effect along the main lobe direction, but might be noise re-radiators for this test. A more definite test has been designed with an l.o.s. signal monitor at the source of transmission.

(S) In conclusion the signal to noise measured on this one-way path test does not indicate that ionospheric propagation effects, exclusive of ionospheric scatter effects, are a source of the Clutter-Related Noise observed on the AN/FPS-95. If further tests finally prove that the primary noise agent is not a hardware problem, but in the ionospheric path or backscatter mechanisms discussed in the introduction, a solution to the dynamic range requirement is readily apparent: a reduction in amplitude of the strong signal imposing the dynamic range requirement in the first place, the clutter. This level is determined by the resolution cell size: the azimuthal beamwidth and pulse length. Nine dB reductions in each of these are easily achieved, based upon previous experiments elsewhere, with no restrictions imposed by the ionosphere. A/D converters required to handle the higher sample rate are also available under the weaker dynamic range requirements. Further design modifications will depend upon the solution of the systems analysis problem at hand and resulting level of prominence of contributing noise agents.

ACKNOWLEDGMENT (U)

(U) The authors wish to acknowledge discussions with other Naval Research Laboratory personnel, MITRE and RCA personnel, and in particular Dr. Robert Rafuse of Rafuse Associates.

SECRET

REFERENCES

1. R. Rafuse, "Observations On The Testing of OTH Backscatter Antennas for Multiplicative Noise", Tech Memo #RATM-73-1, ESD, L.G. Hanscomb Field, Bedford, Mass. 1973.
2. R. Rafuse, "Main Antenna Element Wind Vibration Frequencies", Tech Memo #RATM-73-10, ESD, L.G. Hanscomb Field, Bedford, Mass. 1973.

SECRET

APPENDIX I (U)

(U) At a PRF of 160 pps and a sample rate of 4 kHz, a signal of constant doppler is the series of samples

$$x_m = A_m \cdot \exp(imf 2\pi/25)$$

where $x(m)$ is a complex receiver sample = (in-phase sample) + i (quadrature sample), $A(m)$ is the magnitude of the sample, $m(2\pi/25)f$ is the phase of the sample, and f is doppler/PRF. For a CW signal, $A(m)$ is a constant for all m . For a given f , samples can be coherently averaged by taking an average after adjusting the phase of each sample. If coherent averaging is done and if the noise is uncorrelated from sample to sample, the gain in signal-to-noise ratio obtained by averaging M samples is M .

(U) If the phase is not adjusted, the averaging will yield a signal-to-noise ratio gain of

$$G(M, f) = (1/M) \sum_{m=1}^M \exp(imf 2\pi/25),^2$$

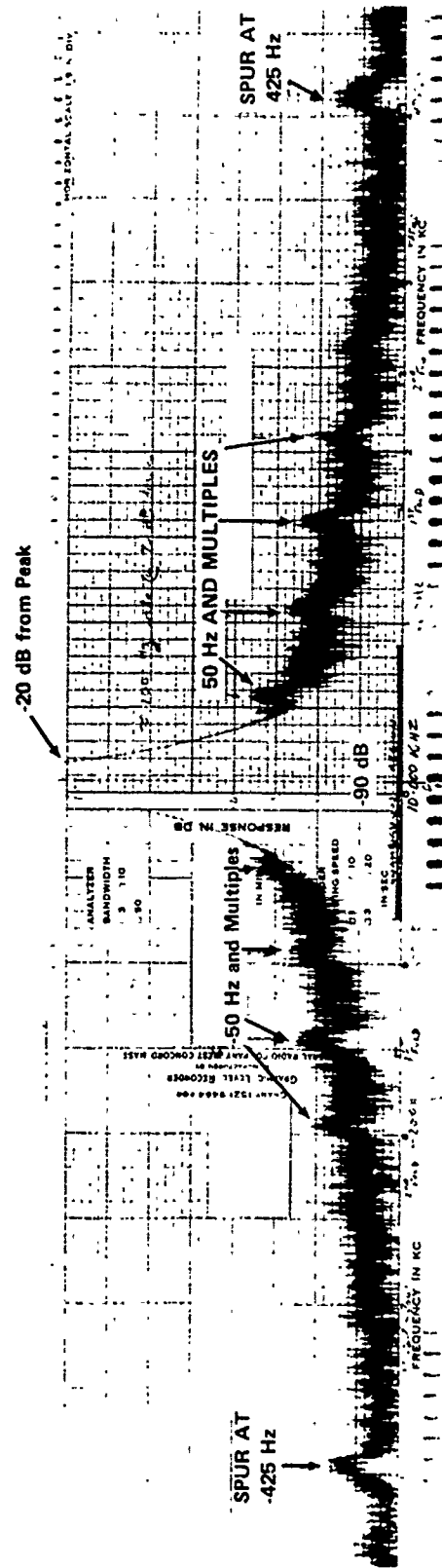
$G(M, f)$ is plotted in Figure A1 for $M = 5, 10,$ and 20 .

SECRET

MECON 30 10N - 115 WORLD WPS - NOV 9 0RS 55M+ 37 FDE-1.00 1071-: 00 F0Z2-1.00
DIPOLY CRFZ
ORDIMRY
NO COLLISIONS
F = 23.500000 MHZ

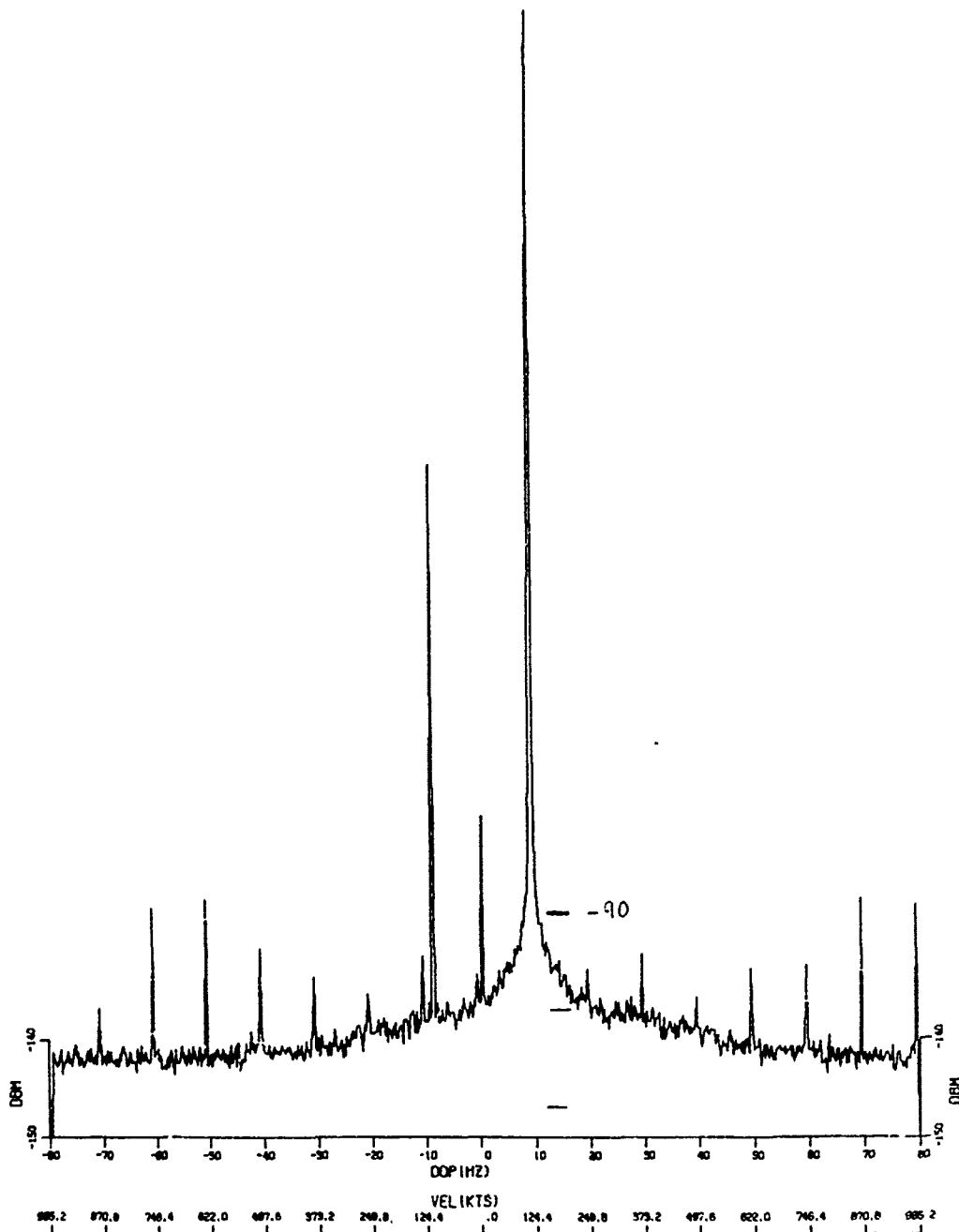


(U) Fig. 1 - Ray trace for propagation at 116° azimuth, and operating frequency of 23.500 MHz. Ionospheric data input to the program is a two-dimension grid from the ITS-NRL propagation prediction program for the month of November.



(S) Fig. 2 - Transmitter spectrum provided by COBRA SHOE personnel. Analysis bandwidth was 10 Hz, so that the noise observed is riding upon the skirts of the filter.

SECRET

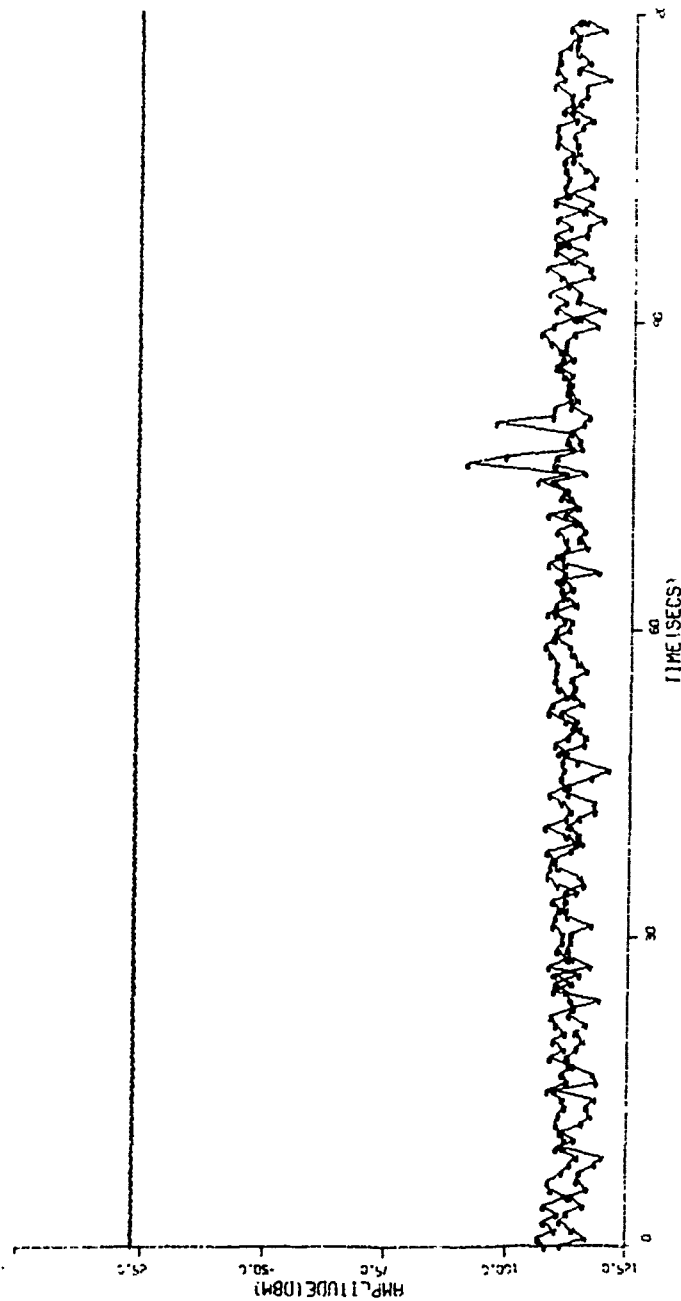


B 3,+20

BM	PRF	I-T	OVLAP	THRESPL	TRUNC	START	FREQ	DAY
13	160.	25.6	1.0	-150.	200.0	21, 5, 5	23500000	11
		5 DATA PT PER	1 PLOT PT					

(U) Fig. 3 - An ensemble average of twenty spectra, processed with a 25.6-second coherent integration time, on a Hewlett Packard synthesizer signal inserted into the receiver front end with a Doppler offset of 10 Hz.

SECRET

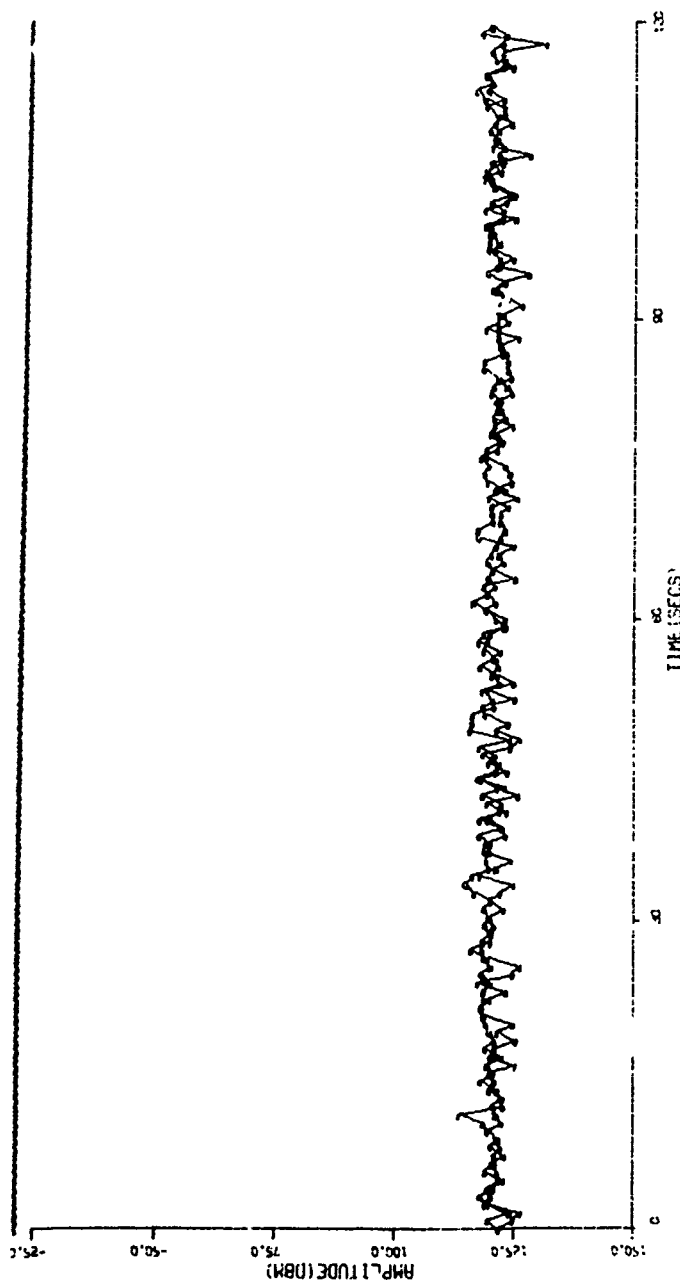


HZ	2	BM, DAY	BIN	FULLWIDTHS	I.T.	FREQUENCY	TIME	MEAN	VAR										
5.0	15.0	13	11	3	10	30	50	70	.8	23500000	21	61.30	23.2	.00					
14.0	19.0																		
-66.0	-61.0																		

CORFNS=-.06-.54 .01 .60 IMNRMS=-108.2 TVAR= 4.3 S-RMS= 84.9
CORFNS=-.12-.36 .06 .61 IMNRMS=-114.2 TVAR= 2.7 S-RMS= 91.0

(U) Fig. 5 - A display of signal amplitude and mean noise levels in a specified band of filter outputs as a function of time, for the same data displayed in Figure 3. The peak signal was found in a band set from 5 Hz, to 15 Hz, using an integration time of .8 seconds.

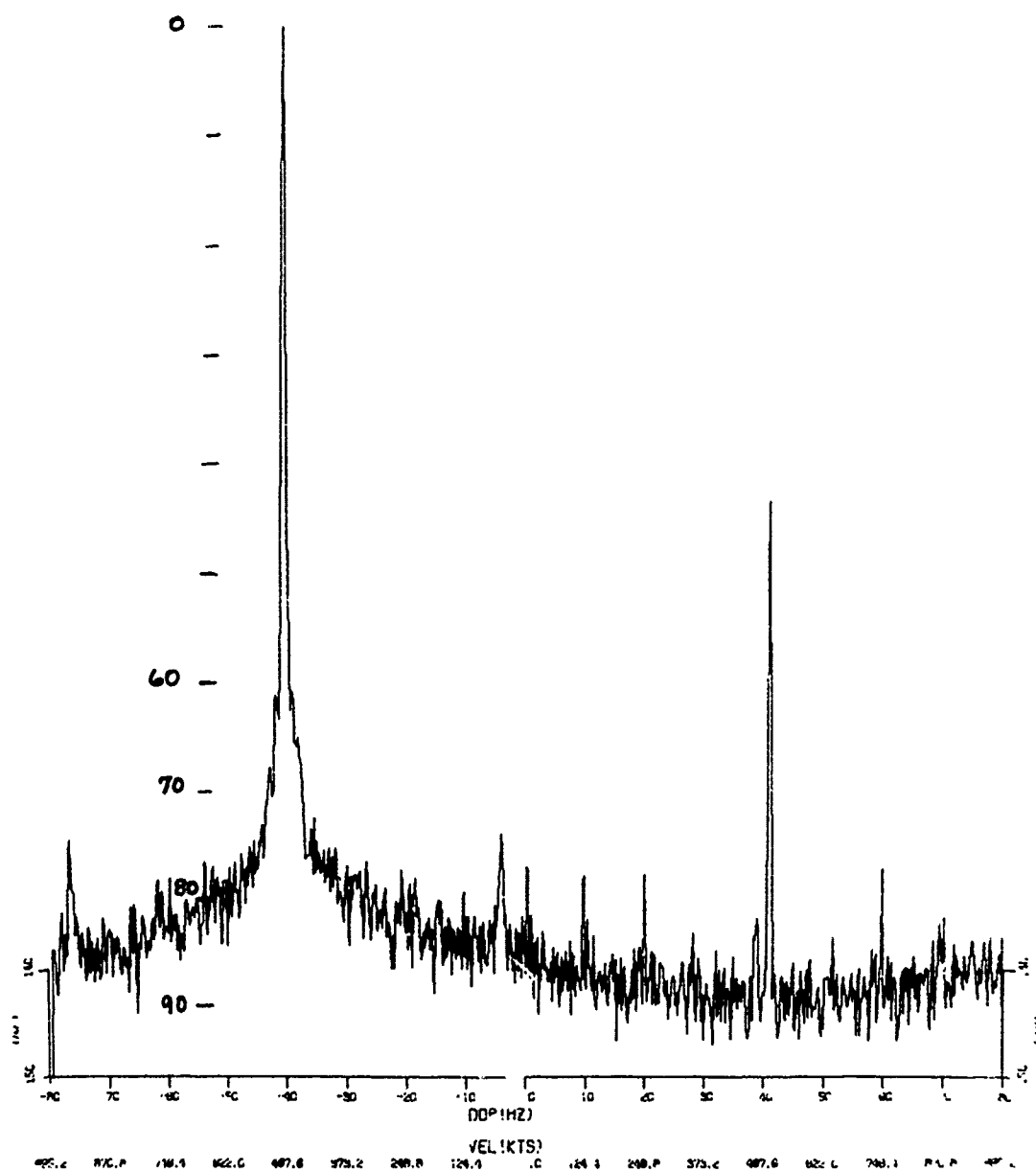
SECRET



Hz	dB	Bin	Freq	Width	I.T.	Freq	Time	S Mean	Var					
5.0	15.0	13	11	1	10	30	50	70	.8	23500000	20.50	0	-21.7	.00
14.0	13.0	CORFNS	...	15	26	.97	.67	IMNRMS	121.0	TVAR	2.6	S/RMS	39.4	
56.0	61.0	CORFNS01	12	.94	.62	IMNRMS	121.1	TVAR	2.3	S/RMS	99.4	

(U) Fig. 6 - Amplitude and noise statistics as in Figure 5, but for a Fluke Synthesizer.

SECRET

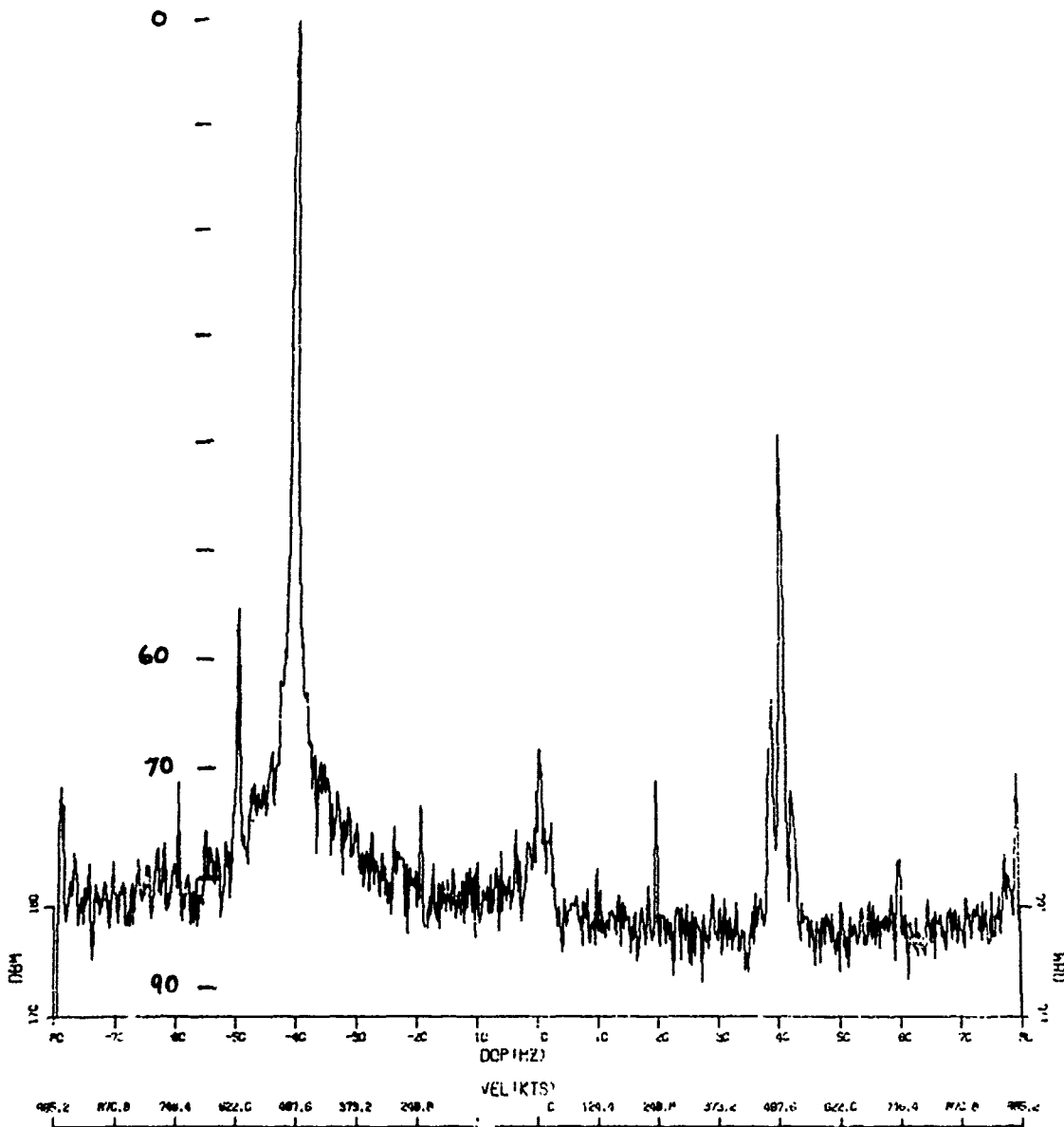


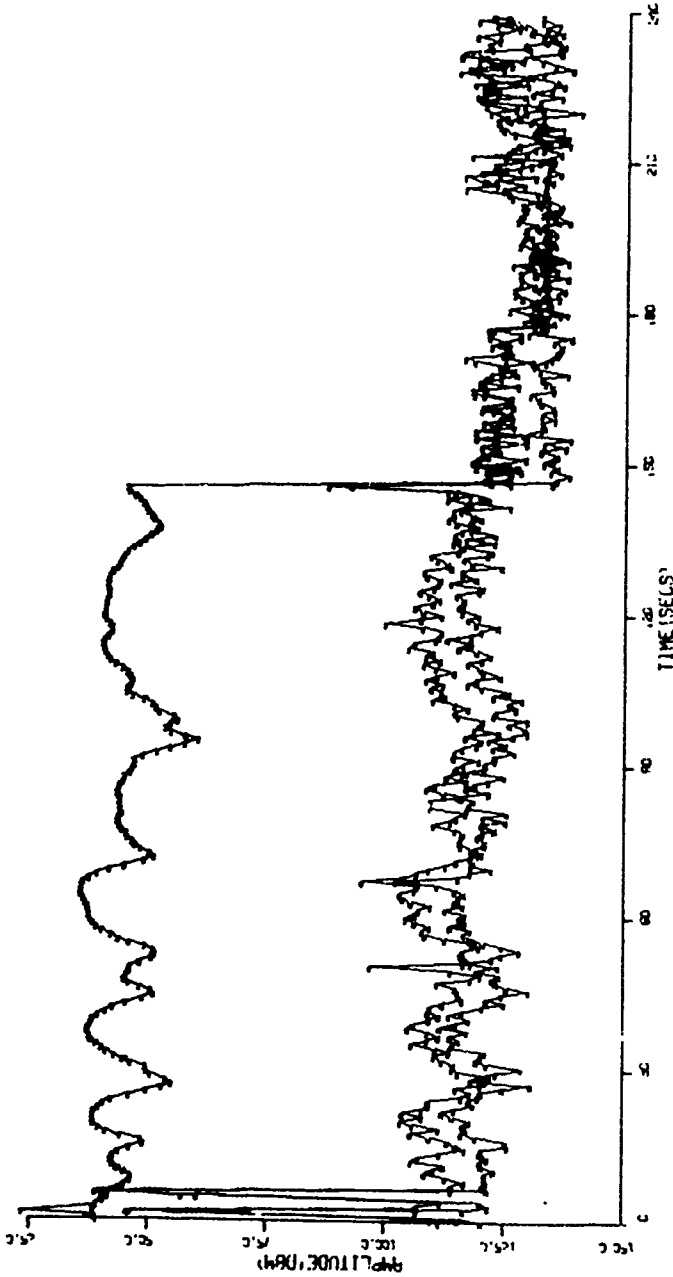
B 3,+4

BY	PRF	I-T	OVLAP	THRESPL	TRUNC	START	FREQ	DAY
13	160.	25.6	1.0	-150.	500.0	8,51,35	23500040	316
		5 DATA PT PER	1	PLOT PT				

(S) Fig. 7 - An ensemble average of four coherent spectra, each of 25.6-seconds integration time, of the COBRA SHOE transmission as received on string 17 of the system antenna.

SECRET

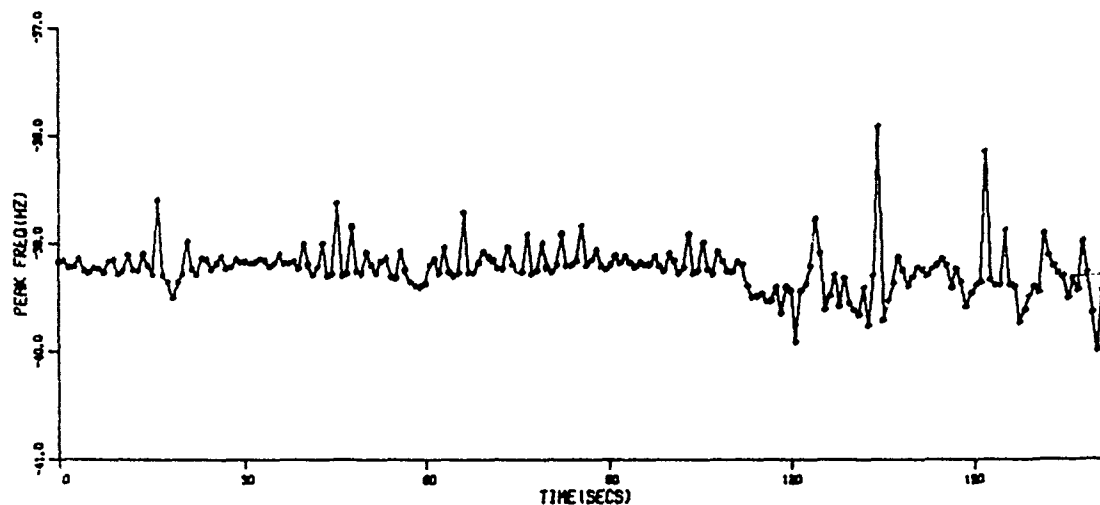




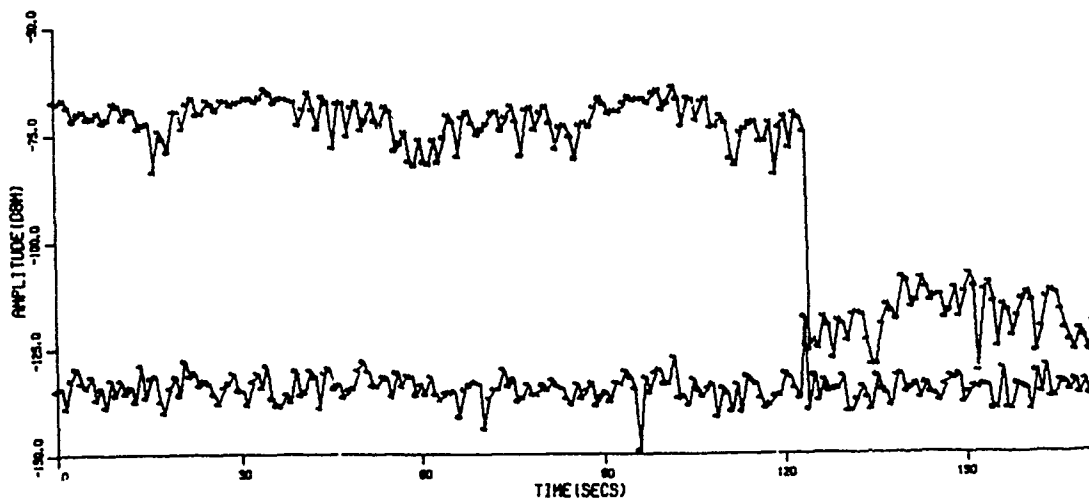
HZ	BM	DAY	BIN	FULLWIDTHS	I.1.	FREQUENCY	TIME	S	MEAN	VAR			
-45.0	35.0	13	315	3	10	30	50	70	.8	23500000	9, 7,34	-42.9	51.29
-15.0	10.0											1VAR=57.7	S/RMS= 21.9
30.0	35.0											1VAR=60.3	S/RMS= 20.5

(S) Fig. 9 - A display of peak and noise statistics as in Figure 5, but for the COBRA SHOE signal received on the system antenna, including a key break. The drop in noise level to ambient is seen during the key break.

SECRET



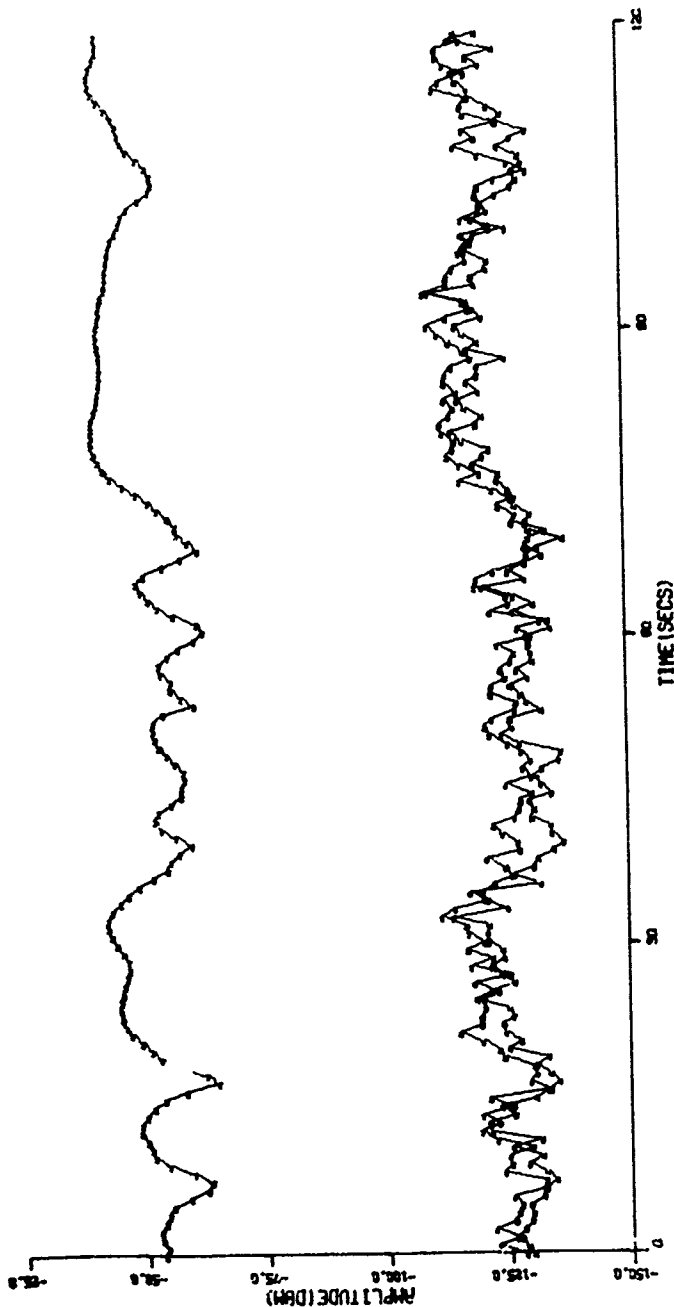
AMP-FREQ CORLN COEFS, .12, -.62, -.12, .64..



HZ1,2	BM, DAY	BIN	FULLWIDTHS	I.T.	FREQUENCY	TIME	S	MEAN	VAR
-35.0, -45.0	13	316	3	0 70 75 80	.8	23500040	9,	1.53	-70.9 25.27
-15.0, -10.0	CORFNS=		.33-.36-.41	.48	TMNRMS=-133.8	TVAR=	3.8	S/RMS=	62.9

(S) Fig. 10 - A display of peak and noise statistics for the COBRA SHOE signal received on the fan dipole test antenna. Note the lack of noise level drop during the key break.

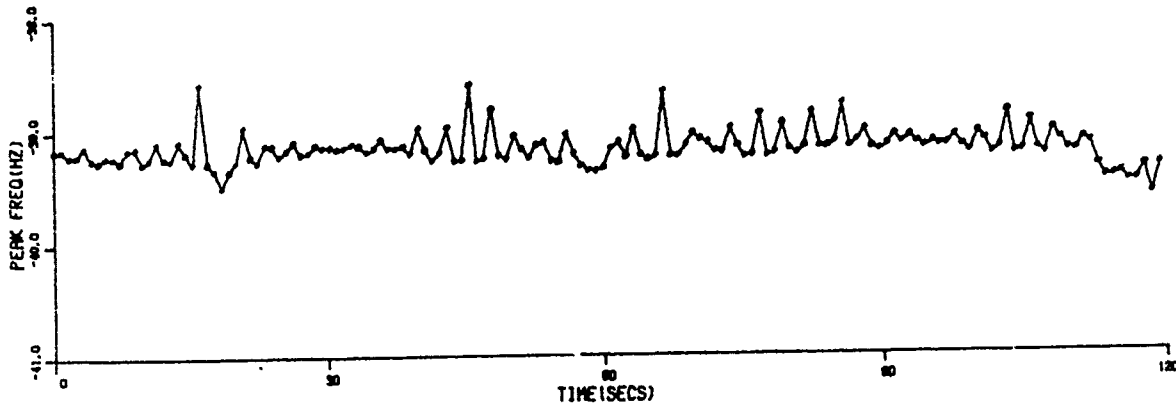
SECRET



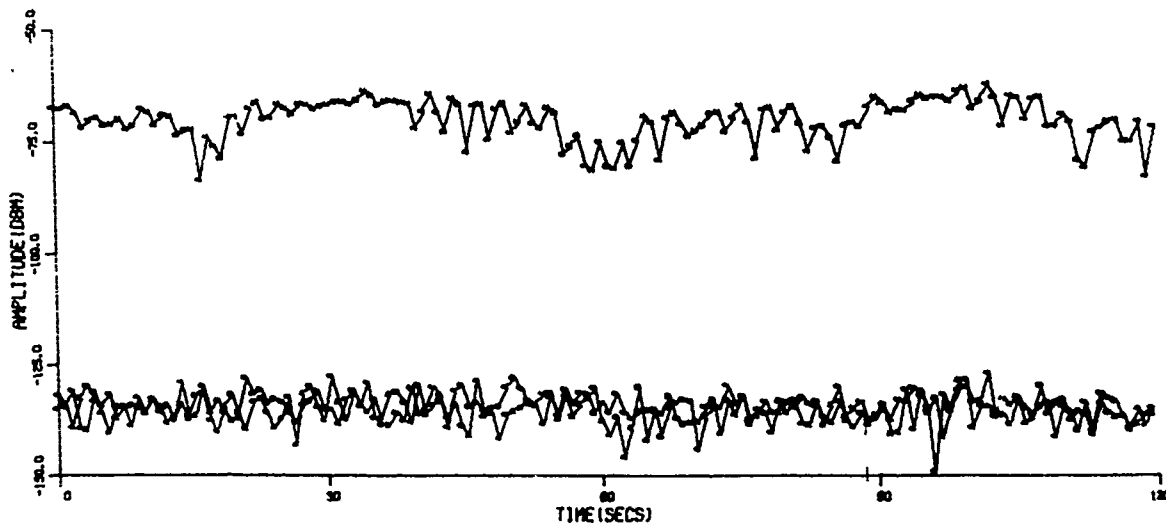
HZ1.2	EM, DAY	BIN	FULLWIDTHS	I.T.	FREQUENCY	TIME	S MEAN	VAR						
-45.0	-35.0	13	316	3	10	30	50	70	.8	23500040	8.51	11	-45.5	7.82
-15.0	-10.0	CORFNS=	.89	-.74	-.74	.90	TMRMS=-119.3	TVAR= 6.9	S/RMS= 73.8					
30.0	35.0	CORFNS=	.90	-.78	-.77	.92	TMRMS=-122.9	TVAR= 6.8	S/RMS= 77.4					

(S) Fig. 11 - Peak and noise statistics for the COBRA SHOE signal as received on a single string of the system antenna, a single sample used to form a range bin.

SECRET



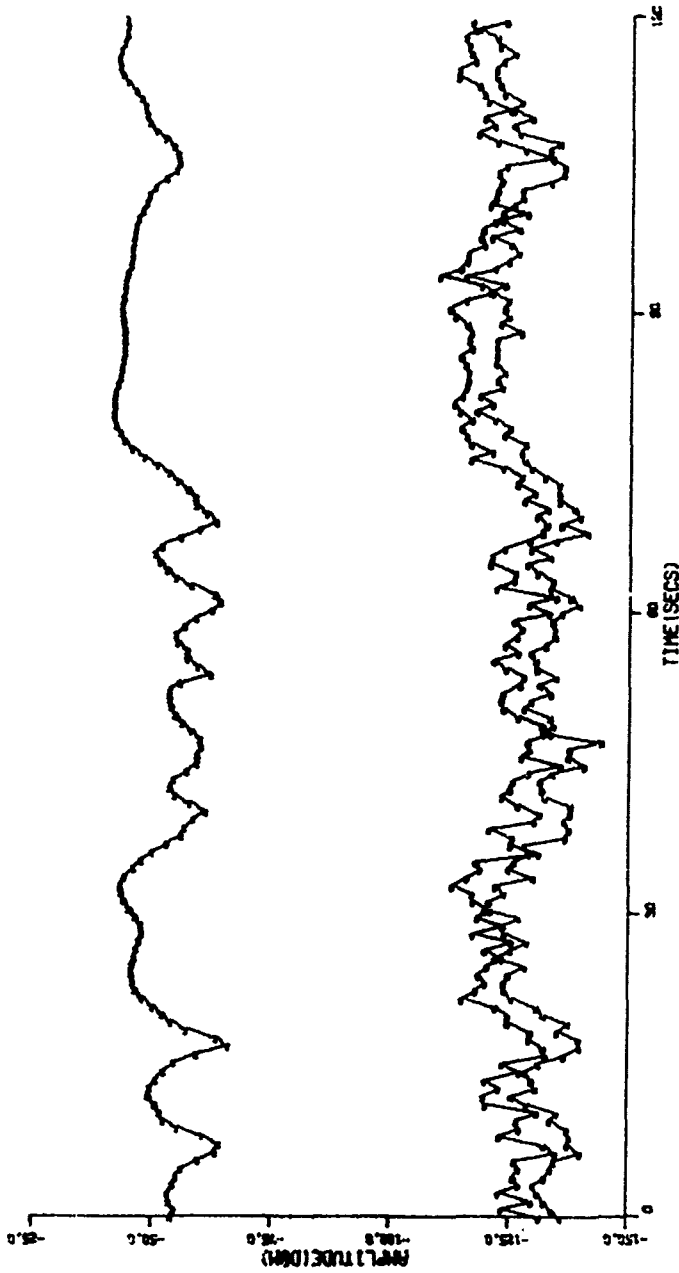
AMP-FREQ CORLN COEFS, -.17, -.65, .12, .77..



HZ1.2	BM.DRY	BIN	FULLWIDTHS	I.T.	FREQUENCY	TIME	S	MEAN	VAR
-35.0,-45.0	13	316	3	0 70 75 80	.8	23500040	9,	1.53	-69.4 4.81
-15.0,-10.0	CORFNS=		.23-.26-.29	.63	TMNRMS=-134.4	TVAR=	3.4	S/RMS=	65.0
30.0, 35.0	CORFNS=		.26-.23-.35	.61	TMNRMS=-135.3	TVAR=	3.6	S/RMS=	65.9

(S) Fig. 12 - Peak and noise statistics for the COBRA SHOE signal as received on the test dipole antenna, a single sample used to form a range bin.

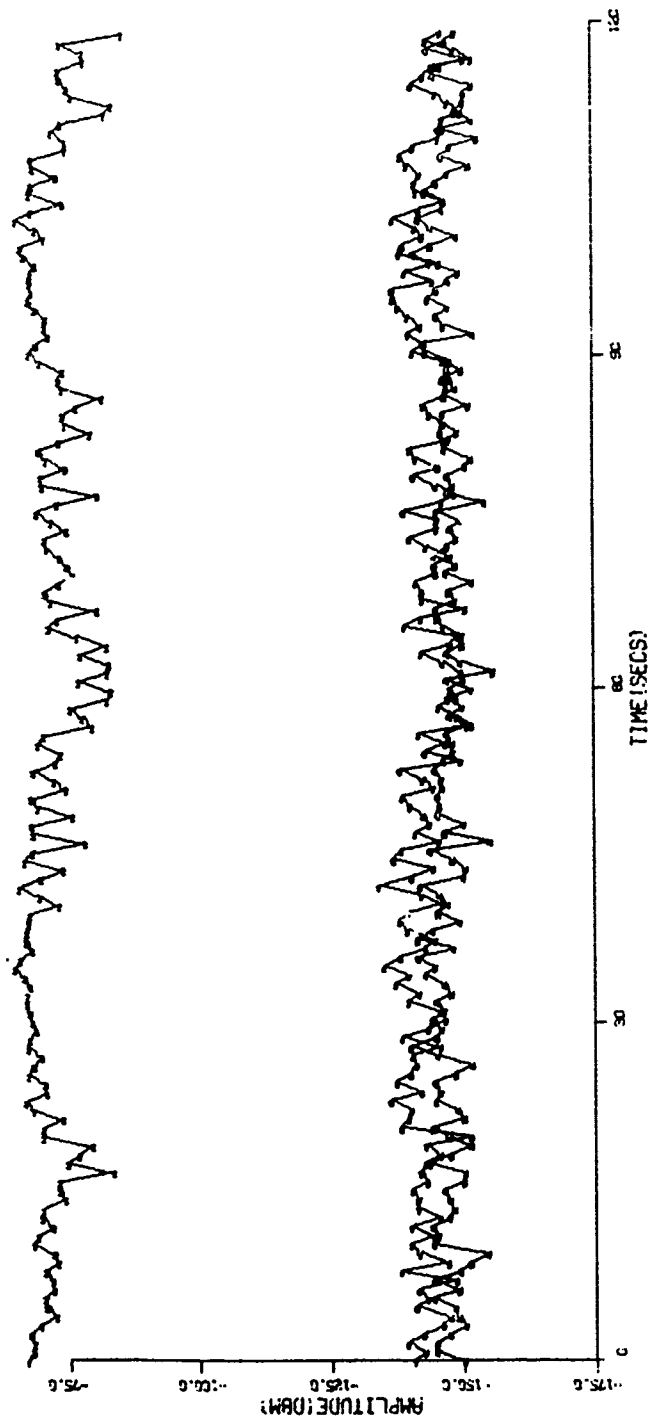
SECRET



HZ1.2	EM.DRY	BIN	FULLWIDTHS	I.T.	FREQUENCY	TIME	S MEAN	VAR					
-45.0	-35.0	13	316	3	10	30	50	70	.8	23500040	8.51,11	-46.2	7.82
-15.0	-10.0	CORFNS=	.91	.76	.75	.92	TMNRMS=-119.8	TVAR=	7.1	S/RMS=	73.6		
30.0	35.0	CORFNS=	.93	.80	.79	.94	TMNRMS=-126.2	TVAR=	7.4	S/RMS=	80.0		

(U) Fig. 13 - The same data displayed in Figure 11, but twenty samples averaged to form a range bin. The signal-to-noise ratio in the -10 to -15 Hz band is virtually the same as the 1 sample/bin case, while that in the 30 to 35 Hz band has improved by 2.6 dB.

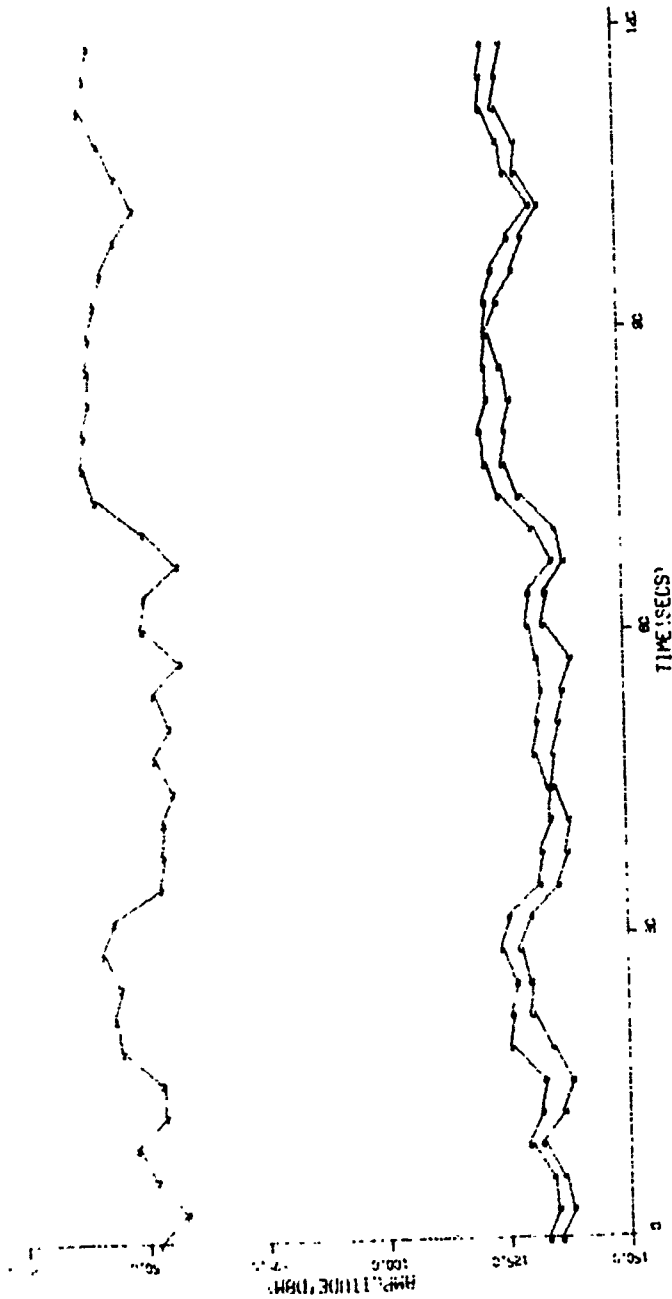
SECRET



HZ	2	BM, DAY	BIN	FULLWIDTHS	L.T.	FREQUENCY	TIME	S MEAN	VAR					
-45.0	-35.0	13	316	3	10	30	50	70	.8	23500040	9	1.52	-70.0	4.77
-15.0	-10.0	CORFNS=	.70	-.55	-.51	.79	TMNRMS=-142.5	TVAR=	4.2	S/RMS=	72.5			
30.0	35.0	CORFNS=	.52	-.39	-.39	.67	TMNRMS=-147.4	TVAR=	3.2	S/RMS=	77.5			

(U) Fig. 14 - The same data displayed in Figure 12, except that twenty samples were averaged to form a range bin. The signal-to-noise ratio has improved in the -10 to -15 Hz band by 7.5 dB, and that in the 30 to 35 Hz band by 7.6 dB.

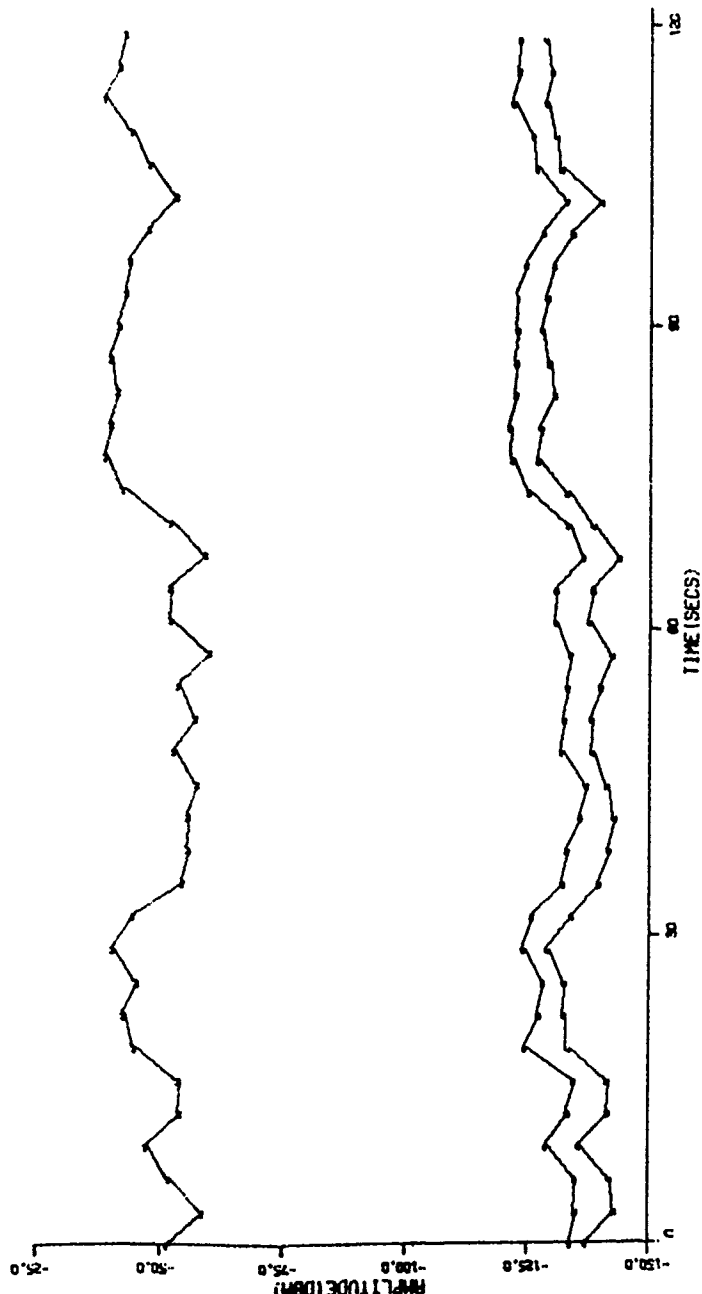
SECRET



EM, DB	BIN	FULLWIDTHS	I. T.	FREQUENCY	TIME	S MEAN	VAR					
45.0	13	316	3	10	30	50	70	6.4	23500040	8.51.16	-44.0	7.29
15.0	10.0	CORFNS=	.96	.75	.76	.98	TNRMS=-	127.2	TVAR=	5.2	S/RMS=	83.2
30.0	35.0	CORFNS=	.96	.75	.75	.98	TNRMS=-	130.5	TVAR=	5.3	S/RMS=	86.5

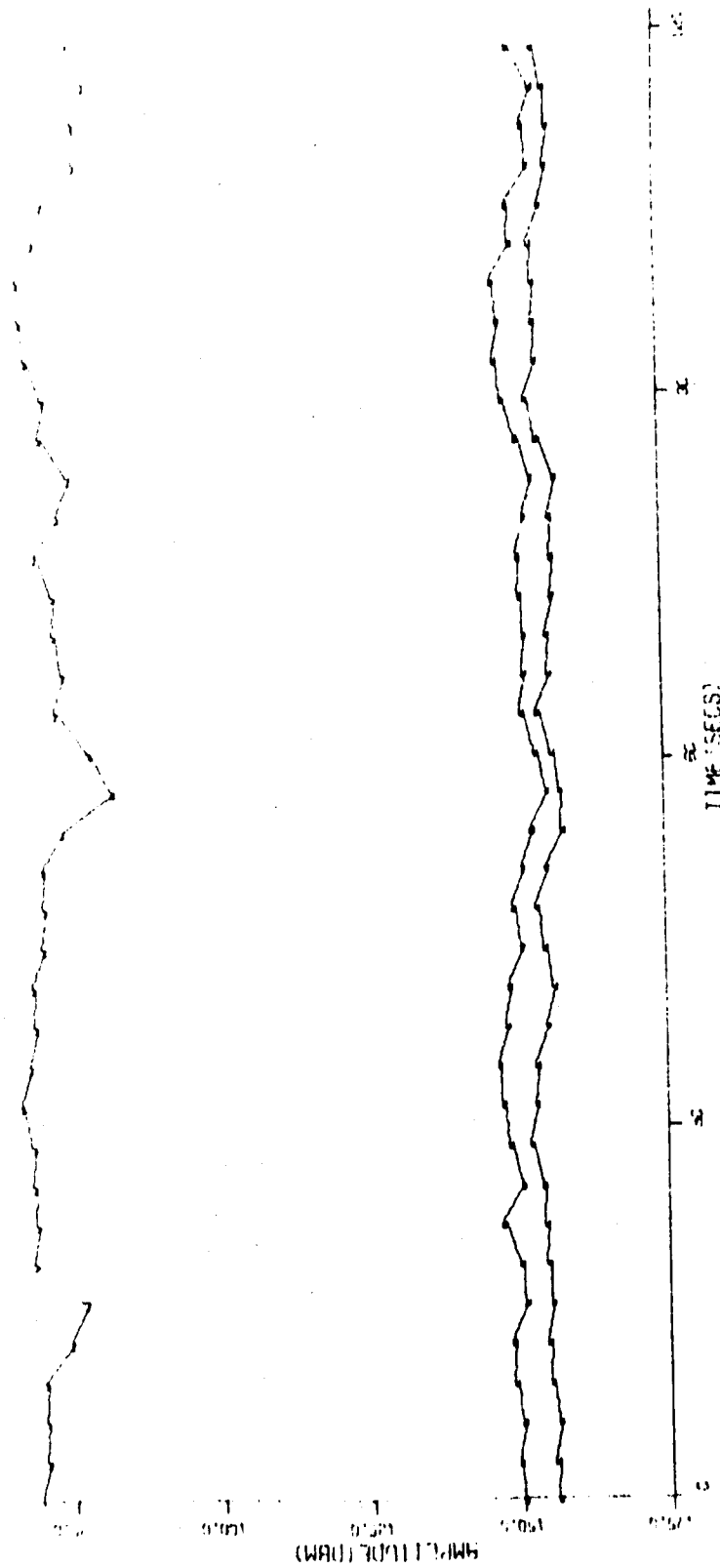
(U) Fig. 15 - The same data displayed in Figure 11, one sample used per bin, but with 6.4 seconds coherent integration time. 9.4 and 9.1 dB signal-to-noise improvement in the Doppler bands results from a 9-dB increase in integration time.

SECRET



HZ1,2	BM, DAY	BIN	FULLWIDTHS	T, T.	FREQUENCY	TIME	S MEAN	VAR					
-45.0,	-35.0	13	316	3	10	30	50	70	6.4	23500040	8,51,16	43.5	7.94
-15.C,	-10.0	CORFNS=	.97	.78	.97	TMNRMS=-127.1	TVAR=	5.8	S/RMS=	83.6			
30.C,	35.C	CORFNS=	.98	.80	.98	TMNRMS=-133.4	TVAR=	6.2	S/RMS=	89.9			

(U) Fig. 17 - The same data displayed in Figure 15, but with 20 samples averaged to form a range bin. Only 0.4-dB improvement in the -10 to -15 Hz band, and 3.5 dB in the 30 to 35 dB band results from sample averaging.



HZ1.2 8M,DRY BIN FULLWIDTHS I.T. FREQUENCY TIME AVEAR: 1.57
 -45.0, 35.0 13 316 3 10 30 50 70 6.4 23500040 0.9 1.57 1.4 1.4 1.4
 15.0, 10.0 CORFNS= .86-.54-.53 .09 TMRMS=151.1 IVAR= 2.1 3.7NS 20.4
 30.0, 35.0 CORFNS= .64-.37-.36 .73 TMRMS=156.1 IVAR= 1.4 3.7NS 25.4

(U) Fig. 18 - The same data displayed in Figure 16, but with 20 samples averaged to form a range bin. 8.6-dB improvement in the -10 to -15 Hz band, and 10.8 dB in the 30 to 35 Hz band result from the sample averaging.

Best Available Copy

MEMORANDUM

20 February 1997

Subj: Document Declassification

Ref: (1) Code 5309 Memorandum of 29 Jan. 1997
(2) Distribution Statements for Technical Publications
NRL/PU/5230-95-293

Encl: (a) Code 5309 Memorandum of 29 Jan. 1997
(b) List of old Code 5320 Reports
(c) List of old Code 5320 Memorandum Reports

1. In Enclosure (a) it was recommended that the following reports be declassified, four reports have been added to the original list:

Formal: 5589, 5811, 5824, 5825, 5849, 5862, 5875, 5881, 5903, 5962, 6015, 6079, 6148, 6198, 6272, 6371, 6476, 6479, 6485, 6507, 6508, 6568, 6590, 6611, 6731, 6866, 7044, 7051, 7059, 7350, 7428, 7500, 7638, 7655. Add 7684, 7692.

Memo: 1251, 1287, 1316, 1422, [redacted], 1500, 1527, 1537, 1540, 1567, 1637, 1647, 1727, 1758, 1787, 1789, 1790, 1811, 1817, 1823, 1885, 1939, 1981, 2135, 2624, 2701, 2645, 2721, 2722, 2723, 2766. Add 2265, 2715.

The recommended distribution statement for the these reports is: **Approved for public release; distribution is unlimited.**

2. The above reports are included in the listings of enclosures (b) and (c) and were selected because of familiarity with the contents. The rest of these documents very likely should receive the same treatment.

J. M. Headrick
J. M. Headrick
Code 5309

Copy: Code 1221 — *CR OK 7/2/97*
Code 5300
Code 5320
Code 5324